Dark Matter in Cosmology

Litsa, Aliki[1], Bovenschen, Stan[2], and Heikamp, Marnix[3]

[1]GRAPPA institute, University of Amsterdam, 11572418
[2]GRAPPA institute, University of Amsterdam, 10639578
[3]GRAPPA institute, University of Amsterdam, 11805188

Abstract

Contents

1 Astrophysical and Cosmological methods indicating the existence of dark matter (Aliki Litsa)

The history of dark matter began in the 1930s, when a Dutch radio astronomer by the name of Jan Oort analyzed numbers and velocities of stars located near the Sun and reached the conclusion that the particular stars appeared to be lacking approximately 30-50% of the matter necessary in order to account for their apparent velocities. In 1933, and shortly after Oort's work, Fritz Zwicky performed similar calculations, and concluded that velocity dispersions in rich galaxy clusters require approximately 100 times more mass in order to ensure that they remain bound. Similar research, including various other astrophysical and cosmological methods, continued more intensely during the following decades, and especially in the 1970s, when researchers attempted to further constrain the existence of such *invisible matter*, using galaxy rotation curves. The following paragraphs contain an overview of the main Astrophysical and Cosmological methods, which established the existence of dark matter in the minds of the scientific community.

1.1 Velocity Dispersion

As we mentioned above, the earliest dark matter indications appeared through calculations related to the velocity dispersion of galaxies, and, in particular, those carried out by Zwicky on the Coma Cluster of galaxies [1]. In the particular paper, published in the 1930s, the velocities of galaxies belonging to the cluster were mentioned to differ by at least $1500 - 2000 \ km/s$, according to various observations. Assuming that the Coma Cluster had reached a stationary state, Zwicky implemented the Virial Theorem as follows:

$$2E_k = -E_{pot}$$

, where E_k and E_{pot} stand for the average kinetic and potential energy per unit mass in the system. The cluster size was approximated with $R \sim 10^{24} \ cm$, while including a total number of around 800 nebulae, each with a mass of $M_n \sim 10^9 M_\odot$. The additional assumption of uniform mass distribution for the contents of the cluster, yields a total cluster mass of $M_{CC} \sim 800 \times M_n \sim 1.6 \times 10^{45} \ gr$. The potential energy of such a cluster is given by: $V = -\frac{3GM^2}{5R}$, resulting in an average potential energy per unit mass equal to $E_{pot} = -\frac{3GM}{5R} \sim -64 \times 10^{12} \ cm^2/s^2$. In addition, the average kinetic energy can be expressed as $E_k = \frac{1}{2}\bar{v^2} \sim 32 \times 10^{12} \ cm^2/s^2$. Using the expression of the virial theorem written above, the final result is:

$$(\bar{v^2})^{1/2} \sim 80 \ km/s$$

. Such a velocity appears to be very small compared to the Doppler effects of at least 1000 km/s measured from observations of the Coma Cluster. The ultimate conclusion that was drawn from the above was that the average density of the cluster, had to satisfy $< \rho > \sim 400 \rho_{lum}$. In other words, the real density had to exceed the density of the observed luminous matter by a factor of 400, in order for the cluster to remain bound. If the density failed to comply to this restriction, the 800 nebulae of the cluster would be bound to ultimately disperse and become independent of each other, thus no longer constituting a cluster of galaxies.

At this point it is important to point out the fact that Zwicky's results, as mentioned above, were extremely preliminary, and failed to convince most members of the scientific community at the time. The main reason for that was that the calculation of redshifts for the galaxy-members of the Coma Cluster demanded the use of a Hubble constant that, in the 1930s, was extremely poorly constraint. Furthermore, the uncertainties for the masses of the nebulae comprising the Coma Cluster, weakened the argument for the difference between theoretically predicted and observed velocities even further. Whatever the inaccuracies, Zwicky's attempts constitute one of the first steps towards the exploration of the dark matter theory, and are, therefore, worth mentioning in our review. Similar calculations, making use of more accurate data, have, since, been performed for many more known large structures of matter in the Universe, since Velocity Dispersion constitutes one of the basic indicators for the existence of dark matter.

1.2 Rotation Curves

The rotation curve argument is another serious indication for the existence of dark matter in the Universe from the early years of research on the topic [2], until today [3], [4]. Such a curve is essentially a diagram of the rotational velocity versus the distance from the center of a galaxy, as presented in Figure 1, and can be better understood by the following simplified explanation.

In the presence of *only* visible gravitational forces, the virial theorem of hydrostatic equilibrium gives:

$$Mv^2 = \frac{GM^2}{R}$$

or

$$\frac{v^2}{R} = \frac{GM}{R^2}$$

As a result, the *Keplerian rotation curve* follows the relation $v \propto R^{-1/2}$. However, the observations do not appear to agree with such a conclusion and, instead of rotation curves which decrease with the distance, they give flat curves, indicating that the velocity has to follow $v \sim const.$ instead. From the virial formula above and with a constant velocity, one can also conclude that $M \propto R$ and, moreover:

$$\frac{dM}{dR} = \frac{v^2}{G}$$

But how can this conclusion be reconciled with the dark matter theory? The essence of the argument supports that the Keplerian curves do, actually, accurately represent reality, but at much larger distances than the ones we are able to observe. Therefore, a logical conclusion indicates the existence of much larger galaxies, where great quantities of dark matter extend far beyond the visible matter, in what can be approximated as a spherically symmetric dark matter halo. The density of such a galaxy can be calculated from:

$$\rho = \frac{1}{4\pi R^2}\frac{dM}{dR} = \frac{v^2}{4\pi G R^2}$$

and, therefore, $\rho \propto R^{-2}$ beyond the visible radius.
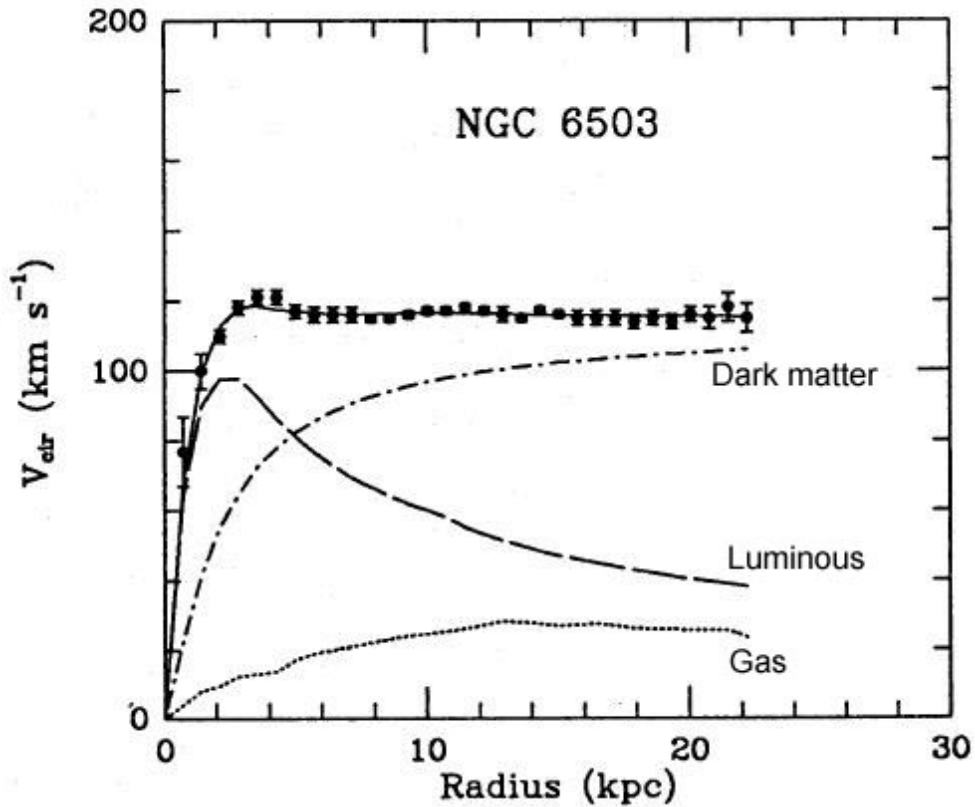
Figure 1: Rotation curve of NGC 6503 [5]

1.3   Gravitational lensing

Another astrophysical method that has been extremely important for the establishment of the dark matter argument is that of gravitational lensing, and especially of the weak gravitational lensing. More specifically, Gravitational lensing is one of the various predictions made in Albert Einstein's theory of General relativity and refers to the deflection of light by gravitational fields, as well as to the resulting effect of that deflection on images seen by an observer. In Figure 3 we can see a simple depiction of the gravitational lensing effect,

Figure 2: Deflection of a light beam originating from a point-like source

in the case of light rays travelling from a distant quasar and being deflected by a galaxy-lens. The result is the creation of two *false images* of the quasar, which are observed from Earth, and give a false perception for the position of the quasar object on the celestial sphere. In Figure 5, w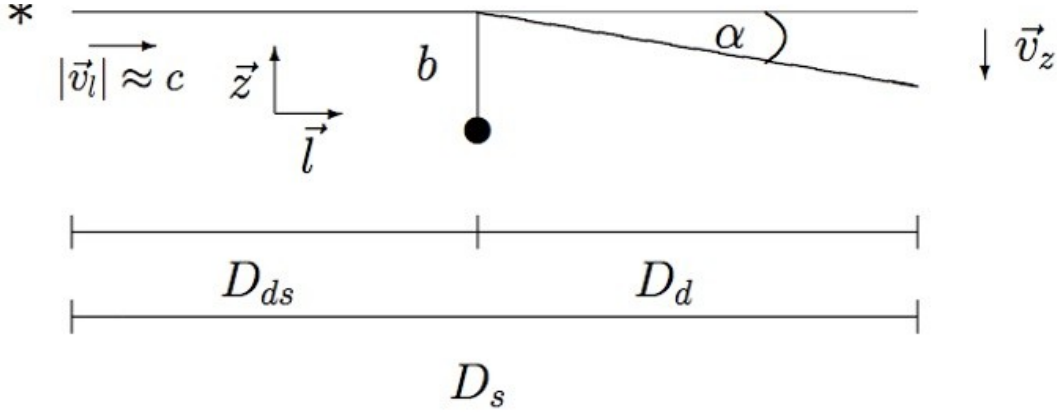e, also, present an example of strong gravitational lensing from Abell S295, where the two "false" images can, also, be observed very clearly. There exist various different types of gravitational lensing, depending of the strength of the effect and on the corresponding degree of image distortion of distant objects, including strong gravitational lensing, weak gravitational lensing and gravitational micro-lensing. More specifically:

- **Strong gravitational lensing**, in which case the mass of the lens is enough to produce multiple images, arcs, or even Einstein rings. Generally, the strong lensing effect requires the projected lens mass density greater than the critical density Σ_{cr}. For point-like background sources, there will be multiple images; for extended background emissions, there can be arcs or rings.

- **Weak gravitational lensing**, in which case the mass acting as a lens causes disfigurements to the background objects that are observed, but is not strong enough to produce arcs or rings.

- **Gravitational microlensing**, in which case the lens allows the observation of sources producing little or no light, due to the collection and beaming of emitted light towards the direction of the observer.

In order to better understand the concept of gravitational lensing, we will attempt to present the simple basis of the argument using Einstein's theory of General Relativity, using light originating from a point-like source. The deflection angle a can be calculated from:

$$\vec{\alpha} = \frac{4GM}{c^2 b}$$

where b is the distance from the point-like source of the beam to the observer.

If we consider the gravitational field as an optical medium with an index of refraction $n > 1$, the particular index is such that the light beam travels slower through the medium than through vacuum, and is given by (Ehlers & Schneider 1992 [6]):

$$n = 1 - \frac{2}{c^2}\Phi = 1 + \frac{2}{c^2} \mid \Phi \mid$$

where Φ refers to the gravitational potential. Furthermore:

$$\vec{\alpha} = -\int \bigtriangledown_\perp n dl = \frac{2}{c^2}\int \bigtriangledown_\perp \Phi dl$$

which contains the integral of the potential gradient perpendicular to the light propagation direction ($\bigtriangledown_\perp \Phi = \frac{d\Phi}{dz}$). Therefore, for a light beam traveling at a distance $b = R_{sun}$ from the center of the sun (which is considered as a point-like source), the deflection angle α is calculated to be approximately 1.7". Further topics that are related to Gravatiational lensing include the lens equation, as well as the phenomenon that is known as the *Einstein ring*. However, such discussion goes beyond the purposes of the particular review.

The method of gravitational lensing can, also, be applied in *Bullet Cluster* observations, where two clusters are undergoing high-velocity collisions, and, subsequently, emit X-rays that have been detected by the Chandra
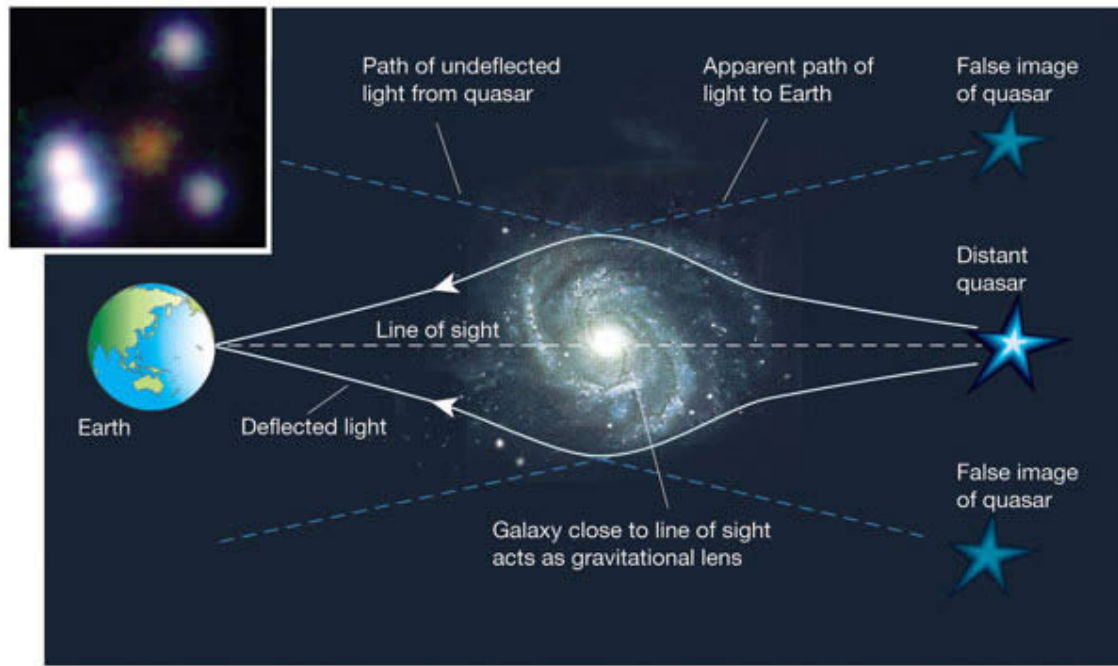
Figure 3: Lensing effect (*taken from https://pics-about-space.com/gravitational-lensing-and-dark-matter*)

telescope. The interested reader can find out more by reading [7, 8, 9]. In images of such phenomena that have been captured, we can observe two different types of material. The *hot gas* is concentrated at the collision front, while some dark matter, confirmed by weak gravitational lensing techniques, is concentrated behind the collision front (Figure 4). We can, therefore, conclude that the dark matter detected in such phenomena, not only exists, but is also collisionless.

Figure 4: Bullet Cluster 1E0657-558. Blue refers to the collisionless dark matter and red to the hot baryonic matter in the collision front. Image provided courtesy of Chandra X-ray Observatory. [10]

Figure 5:   Strong gravitational lensing in Abell S295 [11]

1.4   Baryon Acoustic Oscillations

Having already mentioned various astrophysical methods of establishing the credibility of the dark matter argument, it is time to move on to some cosmological phenomena. The Baryon Acoustic Oscillations are those 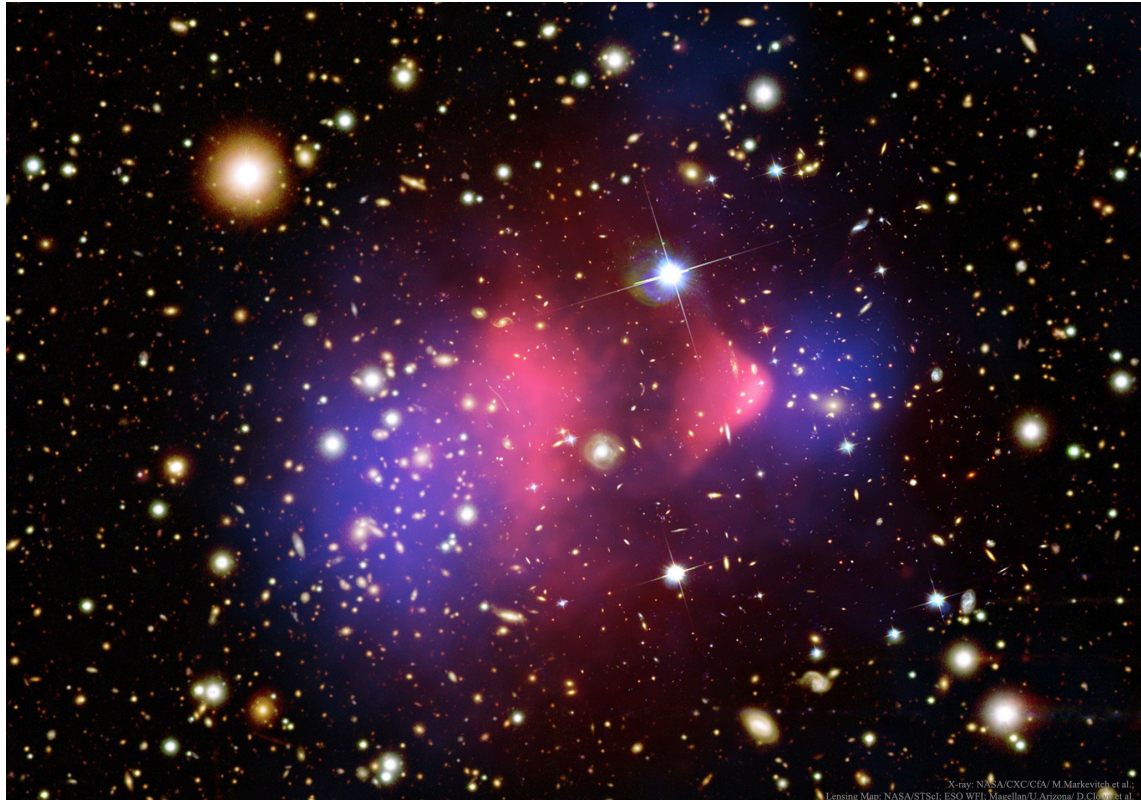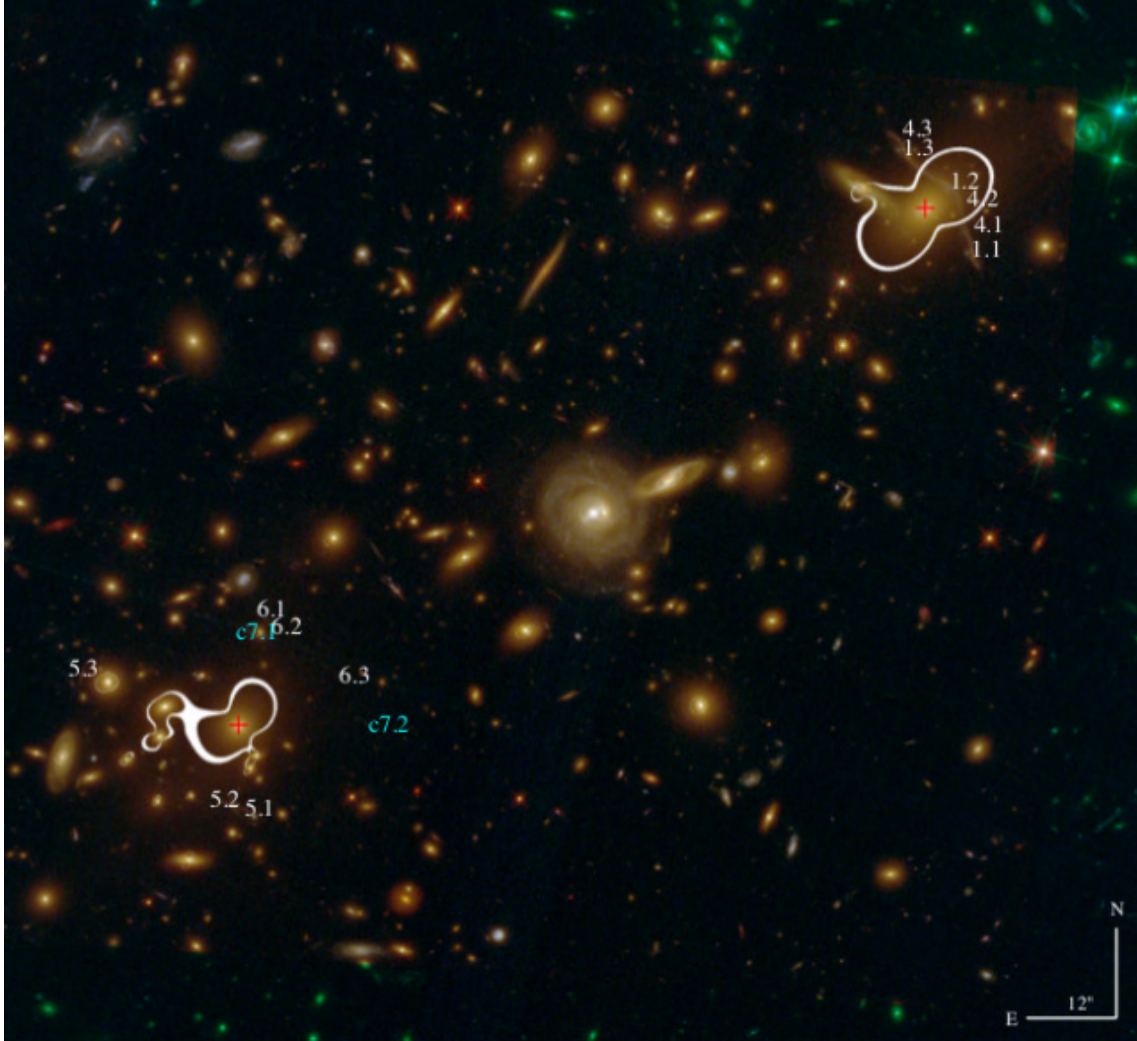that give rise to the various acoustic peaks in the Cosmic Microwave Background power-spectrum [12]. Their creation took place in the Early Universe, before the recombination of electrons and protons (for the formation of neutral hydrogen atoms) and the subsequent release of the CMB radiation. During this early age of the Universe, the various cosmological perturbations caused the excitation of sound waves in the relativistic plasma. Until the time of recombination all the various modes of different wavelength had completed a different number of oscillation periods, a fact that has been "captured" in the CMB power spectrum as the different maxima and minima. While, however, the baryon perturbations travelled outwards in the form of an acoustic wave, the dark matter perturbations grew in place. At the time of recombination, the speed of sound falls rapidly, which results in the end of the sound-wave propagation, at a moment when the baryon acoustic shell has expanded to a radius of $\sim 150\ Mpc$. It is after the time of recombination at redshift $z \sim 1000$ that dark matter perturbations, along with the baryonic perturbations contribute to the creation of all large-scale structures observed in the Universe today. If dark matter failed to exist, and its corresponding perturbations, failed to dominate over the baryonic acoustic perturbations, the resulting structures created would have to be much larger than the ones observed today. We can, therefore, confirm the existence of an additional component, apart from regular (baryonic) matter itself, that is essential in accounting for the cosmological structure witnessed today. Such a conclusion provides a strong ally of the dark matter argument, from a cosmological perspective.
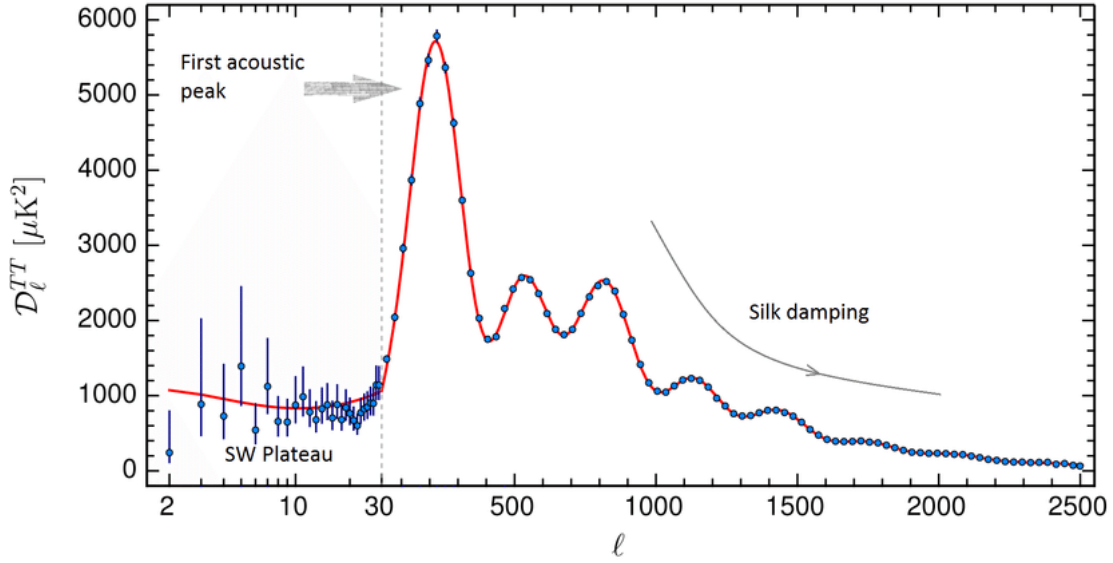
Figure 6: The CMB power spectrum found by the Planck collaboration [13]

2 ΛCDM (Stan Bovenschen)

ΛCDM is a model which combines the components of dark energy and cold dark matter, and the most plausible model of the Universe today. Cold dark matter will be explained in section 4.2. In order to know what amount of dark matter and dark energy we are looking for we can measure the density parameter Ω:

$$\Omega = \frac{\rho}{\rho_c} = \frac{8\pi G\rho}{3H_0^2}$$

The fact that we are measuring a component of the density parameter $\Omega_\Lambda > 0$ (shown in next section) means that there is some dark energy in the universe. Hence we have to use the ΛCDM model.

2.1 Latest measurements from the Planck telescope (Aliki Litsa)

The measurements made by the Planck telescope [13] are constraint using all astrophysical and cosmological methods mentioned in section 1. Some additional constraints are calculated using distance and velocity measurements of Type Ia Supernovae, which are known as "standard candles" for astrophysical observations. The total energy density of all components, considering a flat universe, is expected to be $\Omega_{tot} \sim 1$. According to measurements of the telescope made in 2015, the rest of the components have the following characteristic values:

- The energy density of baryonic matter: $\Omega_b h^2 \simeq 0.02230 \pm 0.00014$

- The energy density of cold dark matter: $\Omega_c h^2 \simeq 0.1188 \pm 0.0010$

- The energy density of dark energy: $\Omega_\Lambda \simeq 0.6911 \pm 0.0062$

- Hubble's constant at the present time: $H_0 \simeq 67.74 \pm 0.46 \ km/s/Mpc$

- The energy density of all matter in the universe $\Omega_m = \Omega_c + \Omega_b$: $\Omega_m \simeq 0.3089 \pm 0.0062$

The values above constitute most of the essential characteristics of the ΛCDM model, and express the contribution of each of the components to the content of the Universe. Some of the problems of the particular model will be discussed in the following sections of the review.

3 Baryonic dark matter (Marnix Heikamp)

We have already seen that there must exist dark matter, but we have yet to determine what kind of matter dark matter consists of. There are various possibilities of matter to consider, some of which will be discussed below, along with the likelihood of dark matter to be composed by them.

The simplest thing to assume is that dark matter consists of ordinary baryons, that we haven't found yet. We have already seen an argument against baryonic dark matter in section 1.4, but we will provide two more:

- **The amount of baryons.** There exist two ways in which we can measure the amount of baryons that are present in the universe. Firstly, we can measure the abundance of light elements, specifically deuterium. This abundance is closely governed by the amount of baryons that exist. Secondly, we can consider the distribution of hot and cold spots in the CMB. Both of these turn out to be in excellent accordance with one another. As we saw, the energy density for baryonic matter is $\Omega_b = 0.02230/0.49 \approx 0.05$, whereas the total energy density of all matter in the universe is approximately 0.30.

- **Various candidates are unlikely**
  - **Hydrogen or helium gas** When hydrogen is frozen, it forms 'snowballs' which would evaporate and thus do not contribute. When helium is in a cool state, it should absorb light that comes from behind it, but this is scarcely witnessed. When there's hot gas, this should emit X-ray radiation, but this is also scarce.
  - **Dusts, rocks or asteroids** More complex elements may create bigger objects, such as rocks or asteroids. However, that would imply that stars should also have higher metalicity than is the case. This is thus not likely. For dust to be present, we should have more blocking of light, which is not abundant. So, also baryonic dust cannot be the constituent of dark matter.
  - **MACHOs.** MACHOs, very low luminosity stars are hard to witness, for apparent reasons. They can be found using gravitational microlensing. Although some have been found over the last decades, it does not nearly come close to explaining all the missing matter in the Universe.
  - **Very massive objects.** The remnants of very massive stars that formed early in Galactic history might form neutron stars and massive black holes. For neutron stars to form, a star usually goes supernova, ejecting many heavy elements into the Universe, which we don't observe. Additionally, the final mass of a neutron star is not high enough to explain all the missing matter. Very massive stars usually end their lives by collapsing into a black hole, which is unlikely to have happened enough to explain the amount of matter that is required.

4   Hot, Warm or Cold Dark Matter? (Stan Bovenschen)

We have seen that dark matter should be non-baryonic and weakly interacting. In addition to the types of dark matter explained in section 3 we can subdivide dark matter even further in three different models: hot, warm and cold dark matter. The difference in these models has to do with whether or not the dark matter particles were relativistic just before recombination. This difference could have a big influence on the matter structures in later stages of the universe. Therefore, we have to look closely at the CMB, which is a direct remnant of the time of recombination, and to the density distribution of matter throughout the universe.

4.1   Hot Dark Matter

Hot dark matter particles are relativistic just before recombination. Around 1980 the hot dark matter model was very popular, since neutrinos seemed to be a good candidate for hot dark matter [14]. People had just discovered that neutrinos were weirdly behaving. Before this time neutrinos were thought of as massless particles. This changed since the discovery of the solar neutrino problem. More specifically, neutrinos are produced in the sun by:

$$4p \rightarrow He + 2e^- + 2\nu_e$$
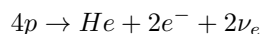
Once we are trying to measure neutrinos on earth we only measure 1/3 of the expected value. The solution to this problem is that neutrinos oscillate, they are constantly changing flavor (ν_e, ν_μ, ν_τ). This is only possible if neutrinos have mass ($10eV < m_\nu < 100eV$). And thus people thought neutrinos could be dark matter. However, hot dark matter has as consequence that small scale structures are damped. The density perturbations in the primordial fluid are damped out by the free-streaming, relativistic neutrinos. This has as effect that the initial structures in the early universe are of size $\lambda_\nu \simeq 40(30eV/m_\nu)MeV$, which is the typical distance a neutrino travels in the lifetime of the universe [15]. Smaller scales, like galaxies, would form later on by fragmentation. We see that this is not the case in our universe and we conclude that λ_ν for hot dark matter is too large.

Another way of answering the question of whether dark matter in the form of neutrinos is a possibility, is by looking at the density parameter, which indicates what the dominant component of the universe is. Ω_ν is

proportional to m_ν [16]:

$$\Omega_\nu h^2 = \frac{\sum m_\nu}{93eV}$$

Since m_ν is very small Ω_ν is very small and so if neutrinos where to be dark matter they would be dominated by the other components of Ω and they would not play a big role.

Still neutrinos are very helpful in the realm of dark matter since they could possibly be produced by dark matter annihilating in the galaxy. This mostly happens inside objects like planets and stars. Neutrinos are the only particles produced by dark matter that could escape from the initial objects [17]. This way we can use neutrino telescopes to observe dark matter.

4.2   Cold Dark Matter

As said before, λ_ν for hot dark matter is too large. A cold dark matter model has, also, been studied extensively, however here we do not encounter this problem. In the particular model, dark matter was non-relativistic before recombination. This has as an effect that, during the radiation era, matter fluctuations where only growing when their wavelengths are larger than the horizon scale. After that, during the matter dominated era, all fluctuations are growing with the same rate. This way large scale structures can arise [14], as mentioned in section 1.4. There are many cold dark matter candidates, the most prominent of which are Weakly Interacting Massive Particles (WIMPs) and Axions, each with different properties.

For WIMPs it is needless to say that they are weakly interacting (otherwise we could observe them easily) and masssive (they need to solve the observed lack of mass). In addition to these obvious properties, they can produce neutrinos, photons, electrons and protons. The latter two can produce more photons through inverse compton scattering. As a result, the CMB could possibly be upscattered by these electrons [17].

Axions are designed to solve the strong CP-problem [18]. Initially the CP-symmetry was supposedly not being violated, until researchers realized that the weak interactions did indeed violate the symmetry. However, we do not know whether the CP-symmetry should or should not be violated for the strong interactions. Experimental research has not been able to give reliable proof of such a violation [19]. There is, however, no reason for it to be conserved, which has led physicists to ask the question as to why it is being conserved. Violation of CP-symmetry causes the axion to have a mass. Both the mass and the strength of the interactions is extremely small, which fits with the predictions of dark matter [20].

Unfortunately the cold dark matter model, also, brings some complications along with it. While on large scales everything appears fine, on smaller scales things are not entirely correct. Galactic velocities on small structures are too large and there are too many clusters of galaxies. In order to correct for those unwanted properties there are two additional dark matter models: the hot + cold dark matter model and the warm dark matter model, both discussed in section 4.3. Of-course, nowadays the Λ cold dark matter (ΛCDM) model, as discussed in section 2, is seen as the most plausible model for dark matter.

4.3   Hot + Cold VS. Warm

We have, previously, seen in this chapter that the hot and the cold dark matter model both have flaws. Hot dark matter arrases the small scales in the early universe. Cold dark matter on the other hand predicts too many clusters of galaxies, in addition to the galactic velocities on small scales being too large. The obvious combination of the two is the hot+cold dark matter model. This model tries to find the right ratio between cold and hot. In 1993 a the following values seemed to agree very well with the observations [21]:

$$\Omega_{cold} = 0.6, \quad \Omega_\nu = 0.3, \quad \Omega_{baryon} = 0.1$$

$$H_0 = 50 \quad km \cdot s^{-1} \cdot Mpc^{-1}$$

where the hot dark matter candidate is taken to be the neutrino. The density parameter Ω_ν gives a total neutrino mass of $m_\nu = 7eV$. Despite the agreement with most observations there are a few exceptions. With the given neutrino mass, galaxies may not be able to account for observations of quasars and damped Ly-α systems at high redshift because they form too late [22]. To tune the results a little further, the total neutrino mass in the cold+hot dark matter model has to be lowered from $7eV$ to $\sim 5eV$. Because the neutrino oscillation's where not quite well understood in 1995, the total neutrino mass was split up into the tau and muon neutrino masses:

$$m_\tau \approx m_\mu \approx 2.4eV$$

This way the calculations for large scales seemed to go quite well. On the other hand, in the particle physics point of view, the hot + cold dark matter model was less appreciable, since the calculated masses where too high to be neutrinos.

This problem can be fixed by introducing a hypothetical particle, the sterile neutrino, which could be a form of warm dark matter. Warm dark matter particles have an even lower cross section than neutrinos and they are less abundant. They have a mass of $\sim 1 keV$. In this case λ_ν is much lower [15]. Warm dark matter is not, yet, excluded from being a possible model for dark matter.

5 Modified Newtonian dynamics (Marnix Heikamp)

So far, we have explained the characteristics of dark matter. However, we have not yet considered the possibility of an alternative theory for gravity. After all, the problem that arises from flat rotation curves can be solved by applying at least one of two different solution concepts: 1. There exists invisible matter 2. Newton's laws do not hold for galaxies [23]. Concept 1 points to dark matter, concept 2 to a different theory of gravity. An example of such a theory is the modified Newtonian dynamics (MOND). It turns out that such a theory can explain the unexpected shape of the rotation curve. In this section, we will describe the theory, and consecutively elaborate on the complications that MOND faces; arising from gravitational waves and the bullet cluster.

5.1 Milgrom's law

Although Newton's laws have been widely tested in high-acceleration environments, they haven't been tested in the realm where objects undergo low acceleration, which happens at the outer edges of galaxies [24]. Thus, we can introduce a constant a_0, with units of acceleration, and state that Newtonian physics applies when $a_0 \gg a$. Then, this paves the way towards a modified expression for the Newtonian force:

$$F_N = m\mu\left(\frac{a}{a_0}\right)a, \tag{1}$$

where m is the gravitational mass of the object, a is the acceleration, and the interpolationg function is:

$$\mu(x) \to \begin{cases} 1 & \text{for } x \gg 1 \\ x & \text{for } x \ll 1 \end{cases} \tag{2}$$

So, in the regime where Newtonian physics breaks down according to MOND, $a \ll a_0$, we find that:

$$F_N = m\frac{a^2}{a_0}.$$

Now, for objects with mass m in a circular orbit (which we approximate the stars in our galaxy to follow), we have that:

$$\frac{GMm}{r^2} = m\frac{(v^2/r)^2}{a_0}$$
$$v^4 = \frac{GMma_0r^2}{mr^2}$$
$$= GMa_0$$

Here, a_0 is experimentally found to be $\sim 10^{-8}$ ms^{-2} [23, 24]. This indeed gives rise to a rotation velocity that is independent of r, such that the rotation velocity is flat, implying there is no need for dark matter.

5.2 Conservation of momentum

We can, thus, see that Milgrom's law, as written in equation 1, solves the problems that arise from the ΛCDM interpretation and which will be discussed in the following sections. However, this is merely a law, which should be derived from a universal force law and, furthermore, does not uphold the principle of conservation of momentum. Let us consider a system in which two masses, m_1 and m_2 are small enough to be in the weak acceleration limit, and in rest on the x-axis. Now, we can express the change in momentum of the system as follows:

$$\dot{p} = \dot{p}_1 + \dot{p}_2 = m_1 \dot{v}_1 - m_2 \dot{v}_2 = ma_1 - ma_2$$
$$= m_1 \sqrt{\frac{F_N a_0}{m_1}} - m_2 \sqrt{\frac{F_N a_0}{m_2}} = \sqrt{F_N a_0}(\sqrt{m_1} - \sqrt{m_2}).$$

We can immediately see that this does not equal 0 when $m_1 \neq m_2$, thus violating the principle of the conservation of momentum. Thus, equation 1 cannot be more than an approximation of a more heuristic force law. Such a law would have to be derived from a variational and action principle, leading to a modified Newtonian dynamics (MOND) theory[1].

To change the dynamics such that they will give Milgrom's law, the classical action provides a good starting point. We describe a system in which a set of particles move in a gravitational field that arises from the matter density, $\rho = \sum_i m_i \delta(x - x_i)$ and is linked to a potential, Φ_N, such that:

$$S_N = S_{\text{kin}} + S_{\text{in}} + S_{\text{grav}} = \int \frac{\rho v}{2} d^3 x dt - \int \rho \Phi d^3 x dt - \int \frac{|\nabla \Phi_N|^2}{8\pi G} d^3 x dt$$

Now, we know that $d^2 x/dt^2 = -\nabla \Phi_N$, which can be used to find $\nabla^2 \Phi_n = 4\pi G \rho$. We can now modify the gravitational action. When we do this, the equation of motion remains in tact, but we will find a different Poisson equation [23]. For the gravitational action, we derive:

$$S_{\text{grav, BM}} = - \int \frac{a_0^2 F(|\nabla \Phi|^2 a_0^2)}{8\pi G} d^3 x dt,$$

where F represents any dimensionless function. We can vary this with respect to Φ, to find:

$$\nabla \left[\mu \left(\frac{|\nabla \Phi|}{a_o} \right) \nabla \Phi \right] = 4\pi G \rho,$$

where $\mu(x) = F(\sqrt{x})$ and $\mu(x)$ still satisfies equation 2. Thus, when $|\nabla \Phi| \ll a_o$, we find that the potential becomes non-linear, which is contradictory to general relativity, which predicts linear equations in the weak-field limit [25]. This means that we can constrain MOND by considering general relativity and gravitational waves (GWs) in particular.

5.3 Gravitational waves

There are two ways in which MOND can alter gravitational wave physics[25]. Firstly, MOND can violate the equivalence principle as it is an acceleration based theory. This would imply that GWs can propagate with a speed that is less than the speed of light . Secondly, as we just saw that the equations are non-linear in the weak-field limit, GWs could then be explained by non-linear equations.

Let's first delve into the first claim. When GWs propagate with $c_g < 1$, where the speed of light, $c = 1$, we must conclude that the arrival times of an electromagnetic signal and the gravitational wave that originate from the same source cannot be the same. However, a recent detection of a GW coming from an inspiraling neutron star binary, of which an electromagnetic counterpart was measured, was made and the time between the arrivals turned out to be 1.7 seconds [26, 27]. This implies that the speed of gravitational waves is equal to the speed of light as that time difference can be explained by the Shapiro time [28]. Additionally, when $c_g < 1$, highly energetic cosmic rays that travel with $v \to 1$ will lose energy via Cherenkov radiation with a rate dependent on $1 - c_g$. Observing such cosmic rays on Earth allows for a lower bound on c_g causing the rate dependence to be $1 - c_g \lesssim 10^{-15}$ [29, 30]. Thus, it is very unlikely that the speed of gravitational waves is less than the speed of light. In some MOND theories, the speed of gravitational waves depends on the gravitational potential and cannot generically be set to 1, thus making these theories inaccurate.

Regarding the second claim on the non-linearity of the gravitational wave dynamics, we can deduce the following. When these dynamics would indeed be non-linear, the GWs that originate from black hole mergers could interact with themselves. However, LIGO's observation of a black hole merger in 2014 showed no such interaction as the observed signal was consistent with predictions made by general relativity [31]. Therefore, we don't require such a scrambling effect, so we would expect that gravitational waves should satisfy linear equations of motions in the weak-field limit.

We can thus conclude that MOND theories must be heavily constrained by the principles arising from gravitational waves. This implies that it becomes questionable whether MOND is an applicable theory, let alone explain the problems that the theory of dark matter attempts to explain.

---

[1]We shall discuss the classical level, and refrain from discussing the weak-field limit, which is more properly described by modified Einstein Dynamics.

5.4   Bullet cluster

The bullet cluster (1E0657-56) merger is a cluster that has given many insights, which we have hinted towards before. Here, we will consider the implications that it has on MOND. At the simplest of levels, this system seems to disprove MOND [32]. In MOND, gravity is expected to traverse the trace of light and would thus not be able to explain the lensing characteristics of the bullet cluster [33]. This happens because the gravitational center is not aligned with the photometric center, indicating that spacetime might be anisotropic [34]. However, bullet clusters also turn out to be difficult for ΛCDM, as the collision velocity (~ 4700 kms^{-1}) is extremely unlikely in this theory [35]. A way around this problem for MOND has been proposed by [36] and has been verified by [34]. Here, a metric is conceived that is comparable to the Schwarzschild metric, with one change. The spatial distancd r is replaced by a distance, $R = r(f(v(r))$. Under certain assumptions, this simplifies to MOND as proposed by Milgrom. This form of MOND can explain the characteristics of the bullet cluster and fits the rotation curve data as well. This may thus explain the missing matter problem [37].

We thus need a special form of MOND to explain the problems that are more generally explained by the theory of dark matter. When also considering the consequences of the recent GWs detection, it becomes tricky to use the theory of MOND as these detections give strong constraints on the possible MOND theories.

6   Numerical Simulations

6.1   Introduction (Aliki Litsa)

The numerical simulation techniques used in dark matter research are closely related to the physics of the Early Universe, as described by the cosmological model of inflation and by that of structure formation seeded by matter and density perturbations. Inflation is the very mechanism that provides the necessary initial conditions in order for the subsequent structure formation to take place, and lead to the creation of all large scale structures observed today. Such conditions include the scale invariant, adiabatic density perturbations, whose growth is first regulated by the radiation itself, and, at later times, by the Dark Matter component of the Universe. The particular perturbations grow during radiation domination, but their growth slows down as they pass the particle horizon. The result is that a characteristic scale is established, which corresponds to the horizon at the moment of transition to the matter dominated era. Since the gravitational potential is the factor which boosts the growth of such matter perturbations, another way of understanding the effect mentioned above, requires an explanation of the way in which the gravitational potential itself evolves. As we can see in Figure 7 the gravitational potential Φ remains constant while the modes remain outside the horizon. Modes with a wavenumber $k \geq k_{eq}$ (where k_{eq} refers to the characteristic wave-number at matter-radiation equality) cross the horizon during the radiation domination era. The amplitudes of such modes decrease as a^{-2}, from the time of horizon crossing, until the time of matter-radiation equality, and, therefore, the particular modes enter matter domination significantly decayed. At this point it is important to point out that, while the perturbation growth proceeds logarithmically during radiation domination, it proceeds linearly (and, thus, more intensely) during matter domination. As a result, modes, like the ones mentioned above, which enter matter domination with a significantly decayed gravitational potential do not contribute as much to the formation of large structures in the Universe. On the other hand, modes which satisfy $k < k_{eq}$, cross the horizon during the matter era and, therefore, correspond to a gravitational potential which faces minimal decay. The particular modes, enter the matter dominated era with a significant amplitude and are, therefore, able to contribute to structure formation. At the same time, dark matter fluctuations, below a certain scale, are washed out by random thermal motions. This free-streaming scale corresponds to the comoving distance a particle can travel during the age of the Universe and satisfies $\lambda \propto m_x^{-1}$ [38].
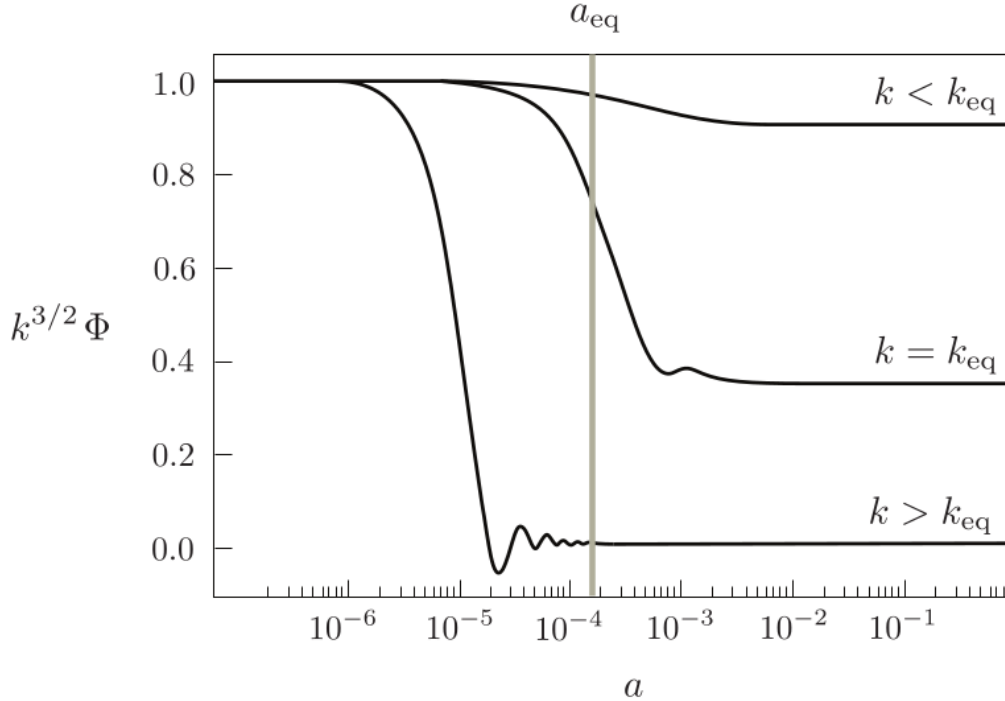
Figure 7: Numerical solutions for the linear evolution of the gravitational potential (taken from Daniel Baumann's notes in Cosmology *https://www.dropbox.com/s/5a6x67n30ssguzv/Chapter4.pdf)*

Having given this short introduction on the processes of perturbation growth and how that affects structure formation, it is time to make the connection with Numerical Simulation techniques and their importance in Dark Matter research. Our conclusions from CMB observations, along with the cosmological theory at hand as described above, indicate that very small structures collapse first and, subsequently, merge to form larger structures. We can, therefore, see that a growth from small to larger and larger objects takes place, ultimately leading to the Universe that is observed today. The baryon acoustic oscillation features, as well as all phenomena related to cosmic scales, emerge from linear or slightly non-linear perturbation growth. As, however, structures get smaller and reach cluster and galactic scales, non-linear growth becomes dominant and the analytical approach of the problem is no longer close to reality. The solution to such a problem is provided by the numerical simulation techniques, which allow the evolution of Dark Matter density fluctuations up to the present day, covering a very large range of length scales (from $\sim 10 \ Gpc$ to $\sim 10 \ pc$). The outcome of numerical simulations is not significantly affected by the composition of dark matter (and by any non-gravitational interactions its ingredients may experience), but rather by the initial velocity distributions of such particles during structure formation. Such distributions do not have a very large effect on large scales, they can, however, seriously influence smaller scales that may be washed out if the particles are highly relativistic (explained in previous paragraph).

The history of Numerical Simulations in galactic interactions should not necessarily be thought of in terms of computational coding processes, since their first steps took place long before such computational procedures were possible [39]. In 1940, Swedish scientist Erik Holmberg conceived a very creative way of visualizing galaxy interactions, by making use of the fact that both the gravitational and the electric force follow the same inverse square law ($F \propto \frac{1}{r^2}$). Holmberg's experiment included 74 light-bulbs, photocells and galvanometers. After measuring the amount of light received by each cell, he manually moved the light-bulbs towards the cell that received the most light, thus simulating galactic motion in the Universe. The years following Holmberg's experiment were characterized by the events of World War II, which boosted progress in all scientific, and especially computational, methods due to the increased military research. However, it wasn't until the early 1970s that numerical simulations in cosmology began to truly prosper, thanks to the newly published cosmological theory of inflation in the scientific community. The initial conditions provided by the particular theory, as explained in the first paragraph of the section, along with subsequent imaging results of galaxies provided by the 3D CfA sky survey (more in section 6.2) gave numerical simulation research the necessary tools for attempting to determine the true composition of the mysterious dark matter component.
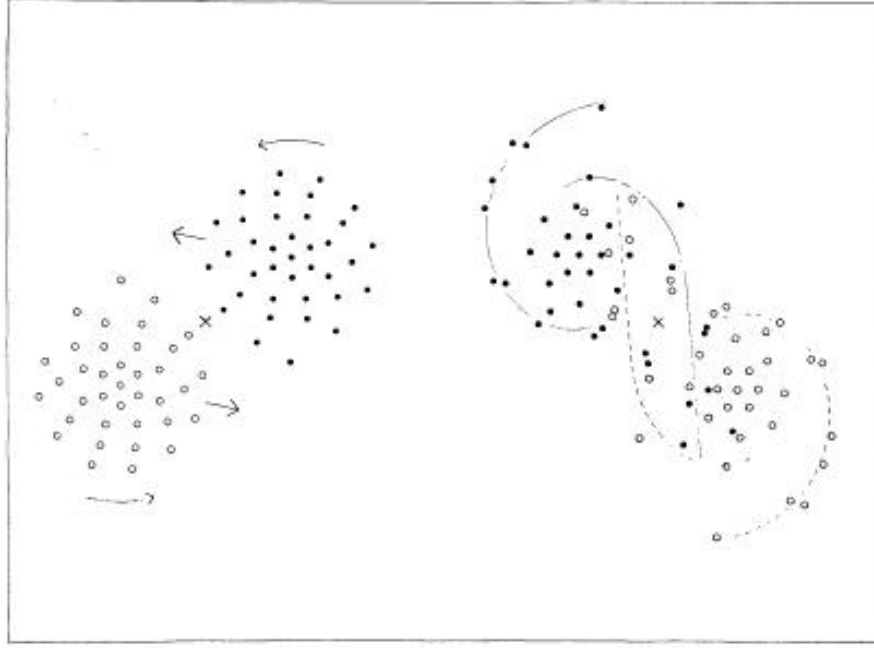
Figure 8: Results of the simulation of a collision between two nebul. Left panel: two disky galaxies approaching. Right panel: after the collision. From Holmberg (1941) [40]

At this point it is important to briefly discuss the particular numerical simulation methods used in order for the result mentioned above to be achieved. In general, cosmological numerical methods include N-body particle simulations, where the gravitational evolution of the particles is determined by the Poisson-Vlasov equations, in a coordinate system which is comoving with the mean expansion of the Universe. The two main techniques include [41]:

- The *Tree Code* technique, where particles are organized in a hierarchical system, depending on their contribution to the gravitational field. More specifically, particles that are very distant from our space-time point of interest, and, therefore, have very low contributions to the gravitational potential of the particular point, are related to low order terms in a multipole expansion of the mass distribution. On the other hand, particles that are closer correspond to higher order terms of the same expansion.

- The *Particle Mesh* method, where particles are placed on a mesh, in order for a density field to be formed. Adapting the particular mesh according to the needs of the problem leads to the formation of high and low density regions.

Such techniques are used for dark matter research in many different scales, from cosmic scale Baryon Acoustic Oscillation simulations to halo simulations in galactic scales. The results of the particular simulations are compared to results from gravitational lensing and CMB observations, in order for conclusions to be drawn.

6.2   Excluding Hot Dark Matter with Numerical Simulations (Aliki Litsa)

As we have, already, mentioned in section 4.1, Hot Dark Matter does not constitute a viable candidate for the explanation of the Dark Matter properties and effects. Despite their limitations and early stage of evolution, numerical methods in the 1980s played the dominant role for the final dismissal of the HDM model (at least in the case of neutrino dominated models).

In the introductory discussion of this section, we already mentioned the dependence of the free-streaming scale λ_f from the mass of the candidate particle m_x as $\lambda_f \propto m_x^{-1}$. For the case of Hot Dark Matter, the mass of the neutrino candidate $m_x \sim 30 \ keV$ corresponds to a free streaming scale that reaches the size of a large galaxy cluster. Since all dark matter fluctuations under the particular scale are damped, scales smaller than large galaxy clusters have to be washed out of the Universe, if, indeed the HDM model accurately represents reality. Despite being intuitively appealing, such an explanation has to be supported by additional computational evidence, in order for the Hot Dark Matter model to be properly rejected.

The imaging data necessary in order for the numerical simulation efforts to be set in motion were provided in 1980s, by the 3D CfA redshift survey, which offered information on the positions of a large number of

galaxies. During the same decade, various research groups [42], [43], [44], [45] created numerical simulation codes with the purpose of modelling structure growth from the initial conditions of inflation until today. Their goal was to compare their results to data collected by the CfA survey itself, and determine whether the HDM model could be considered a reasonable dark matter model, based on its effects on structure formation on large, as well as small scales. Such numerical simulations of non-linear clustering showed that super-cluster collapse in a HDM Universe must have occurred quite recently at $z_{sc} < 0.5$. However, limits on galaxy ages acquired from various globular clusters and other stellar populations indicated that galaxy formation has to have taken place before $z \sim 3$. Moreover, since quasars are associated with galaxies, as is suggested by many observations, the abundance of quasars at $z > 2$ was also inconsistent with the top-down neutrino dominated scheme in which superclusters form first: $z_{sc} > z_{gal}$.

Figure 9 presents three HDM models, two CDM models, as well as actual observations made by the CfA survey [46]. As we can easily conclude from the plot, HDM simulations provide a rather different Universe density distribution compared to the one we can actually observe. As mentioned in the previous paragraph, the clustering scale in the case of Hot Dark Matter exceeds the observed scales of galaxy clustering [45], resulting in a much more clustered pattern than the one provided by observations. The reason behind such an effect lies in the fact that, in the case of HDM, the formation of galaxy superclusters, in regions where collapse has taken place, occurs before everything else, due to the very large characteristic scale that is imprinted at horizon crossing (as explained in section 6.1).
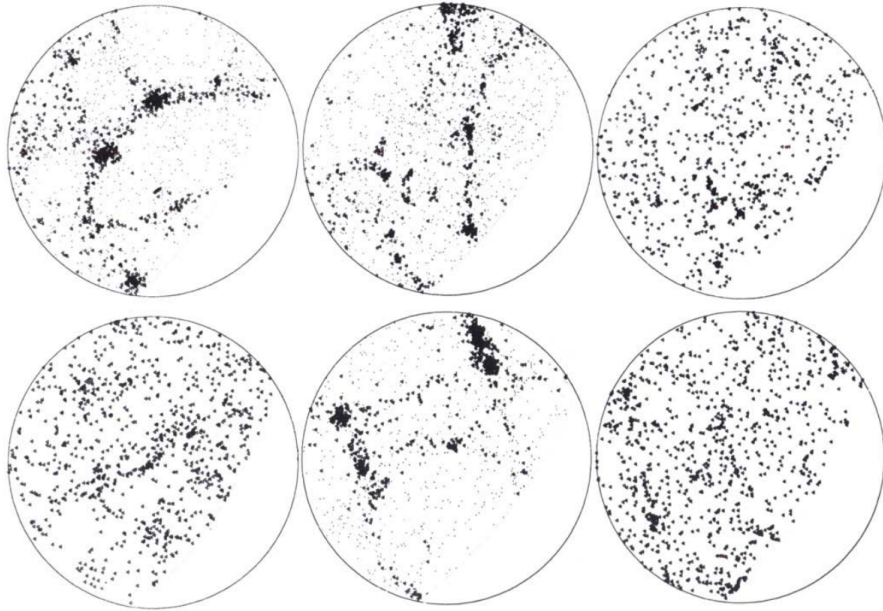

Figure 9: Three HDM models (middle top, middle-bottom and right-bottom panels), two CDM models (left top and left bottom panels) and CfA survey results (right-top) [38]

Further numerical simulations performed during the 1980s [47] made use of the (non-linear) *Pancake model* of Galaxy formation [48], according to which galaxy clusters are created first after the Big Bang, and subsequently fragment into galaxies. The term "pancakes" refers to the thin, dense condensations of gas that are formed from the growth of small inhomogeneities in non-linear gravitational instability theory. After their creation, these condensations, are compressed and heated by shock waves, which leads in their fragmentation into gas clouds. Galaxies and their clusters are formed due to the clumping of these gas clouds. The results of the particular simulations showed that at least 85% of the baryons are so heated by the associated shock that they are unable to condense, and, therefore, unable to attract neutrino halos and form galaxies. This constituted a serious problem for the hot dark matter argument, since, when taking into consideration the primordial nucleosynthesis constraint $\Omega_b \sim 0.1$, baryonic matter does not be suffice for the production of enough structures which can account for the luminosity observed in the Universe.

Despite any inaccuracies related to the possibly flawed observations of the CfA survey, as well as uncertainties related to galaxy formation, the evidence against the Hot Dark Matter argument were, indeed very convincing from these early stages of dark matter research.

6.3   Effect/Complications of baryons on Numerical Simulations (Stan)

Previously in this chapter we have seen several implications where numerical simulations are needed in our search to dark matter. Dark matter simulations usually are simplified by doing simulations with the dark matter component only. Once we know how this single component universe works other components are added. Now, to make a simulation of dark matter only is relatively easy because dark matter does not, or barley, interact. Therefore, not taking in account interactions is a pretty good estimate, yet not entirely correct since the dark matter distribution is coupled to the baryonic distribution in the universe. Once adding the baryonic component we need to take into account not only the interactions baryons have with eachother but also with dark matter. We know that baryons interact strongly in different ways, due to baryons galaxies can and all other known structures can arise. We need to know exactly how baryons behave throughout the universe in order to be able to make a model with the baryonic component. This model will tell us more about the distributions of dark matter since the to components are gravitationally bound. However, modeling all the baryonic matter of the universe brings some complications with it.

6.3.1   Baryonic matter in hydrodynamics

Baryonic matter can be treated like a fluid when the mean free path of a particle is much smaller than the length scale of the fluid: $\lambda_{mfp} << L$. Also collisions have to happen frequent enough for the fluid to have a distribution close to Maxwellian. This is the case for baryonic gass in most parts of the universe. Since we can neglect viscosity but not the magnetic field of the interstellar medium we have to deal with an ideal magneto-hydrodynamic fluid. This way we can explain several characteristics of baryonic matter in galaxies. The spiral arms in galaxies for example arise by the Parker instability. Imagine patch of gas with frozen in magnetic field lines where gravity is in the downward direction. Now we insert a perturbation (see figure ?), the magnetic field lines are bend. The gas will 'stream' along the field lines to the side, as a consequence the middle, perturbed, part will have a lower density an become buoyant. The perturbation grows larger and the gas separates to both sides of the perturbation. A gap between two spiral arms arises.

Since most of the matter in the universe is in the form of gas in the interstellar medium (ISM) we do not necessarily have to look directly to the mass distribution of more compact objects like stars. Indirectly however, stars and other baryonic objects are influencing the ISM constantly. Supernovae, for example, inject an enormous amount of matter in the ISM. The evolution of the ISM throughout the years has to do with many parameters, this is hard to model. Therefore techniques are developed to make calculations easier. The Smoothed Particle Hydrodynamics approach is an example of such a technique, which will be explained in the next section.

6.3.2   Smoothed Particle Hydrodynamics

Once can distinguish two different reference frames for modeling a fluid-dynamic problem. We have the Eularian approach which has its reference frame at a fixed point in space and the Lagrangian approach which has a reference frame that is co-moving with a fluid element. In Smoothed Particle Hydrodynamics (SPH) the Lagrangian we mainly use the Lagrangian approach.

7   Physics beyond the CDM model (Marnix Heikamp)

7.1   Problems on small scales

Recently, we have seen that deviations from the CDM model need to be made to fit the found data. These deviations have implications on the structure and evolution of various cosmological systems and are thus topic of debate amongst atronomers. These discussions focus on the impact that baryons have on the dark matter models that exist, and more generally the interplay between the physics that govern the behaviour of both types of matter. We will first look into the observations, or hints towards physics that extends the CDM model, that have recently been made. The authors of this review expect the reader to have a basic understanding of galaxies and halos, which could alternatively be obtained by reading section 3.2.1. from [49].

7.1.1 Cusp/core problem

7.1.2 Missing satellites problem

7.1.3 Too big to fail

7.1.4 Tully-Fisher relation

7.2 Mass of galaxies and dark matter halos

We have just been exposed to four problems that are frequently recurring in literature on problems with CDM. Though it could be the case that these problems are not connected, we aim to find a common interpretation that may explain multiple, or all, stated problems. We find such a solution in the relationship between the masses of the dark matter haloes and the associated galaxies. This relation is especially uncertain on small scales [49].

The last three problems arise as a consequence of the mapping between between the observed behaviour, specifically the kinematics, of baryons and the halo mass. We find a discrepancy between the halo that is simulated from CDM and the observed abundancy of galaxies. So, in essence, the problem at hand reduces to a counting problem. The former conclusion holds when the current mapping is correct. When this is not the case[2], the main problem preduces to the cusp/core problem. We know that the ratio for the virial velocity to the velocity of the baryonic tracer is higher in cored halos, so when we know which halos inhabit which galaxies, we would be able to confidently interprete galaxy abundances. I.e., we would know whether we would actually have a counting problem or a cusp/core problem.

It is worth mentioning that when we would be more confident about how to compare galaxies with halos, we would be able to get to the root of the cusp/core problem [49]. The amount of energy that is required to move dark matter towards the edges of a galaxy depends on the characteristics of the portential well, and thus on the halo mass. So, when we would know more about the relation between the galaxies to the halos, we would be able to (dis)prove a CDM + baryon physics interpration, that can explain the dark matter densities as a function of the galaxy mass. This gives rise to a sense of urgency to find limits on the halo mass.
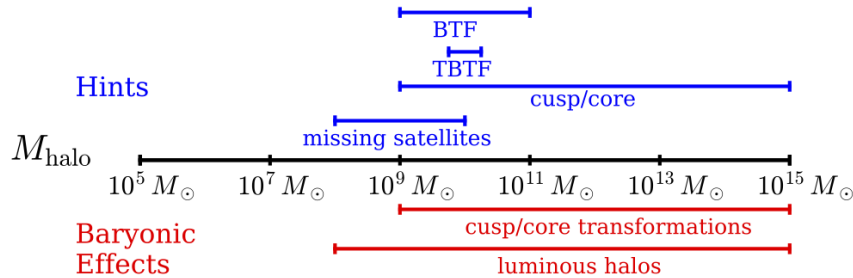

Figure 10: Above: An overview of the various halo masses where hints towards deviations from ΛCDM have been found. Below: An expectation of the range in which baryons are expected to have influence on the structure and evolution of galactic halos [49].

In the top part of figure 10, the different hints towards CDM being an inaccurate description of dark matter at mass scales in the range $10^{9-15} M_\odot$.

7.3 Considering baryonic matter

The four issues that were put forth in the previous subsection have sparked immense interest from both particle and astrophysicists. Together, the people in these fields have come up with many dark matter models that attempt to adapt dark matter halos with $M_{vir} \sim 10^{8-15} M_\odot$. These models mainly consist of predictions that disregard the impact of baryons, for reasons explained in section 3. We have readily seen that baryons have a minor contribution to the energy budget of the system, but they do have an import contribution to the dynamics of a system. Thus, we should consider baryons when extending the CDM model to explain the aforementioned problems that arise. We shall thus consider how considering baryons changes all of the mentioned problems.

---

[2]This could for instance occur due to systematic issues or due to a more fundamental error in the CDM simulations, giving rise to the dark matter mass-profile.

7.3.1 Cusp/core problem

7.3.2 Missing satellites problem

7.3.3 Too big to fail

7.3.4 Tully-Fisher relation

7.4 Future outlook

Slowly, though steadily, more and more studies are investigating this contribution of baryons to the theory of dark matter. Two astronomical systems are frequently used: isolated dwarf galaxies and Milky Way like galaxies. The former is chosen as the computational costs for a high spatial resolution result is relatively low compared to more massive systems. Considering that hydrodynamic simulations are, when important processes such as radiative transfer are ignored, at least an order of magnitude more complicated to execute than dark matter-only simulations [49]. This makes the choice for isolated dwarf galaxies apparent. Studying Milky Way like galaxies is relevant due to the missing satellites and TBTF problems [49].

One of the more noteworthy recent findings on this topic is that including baryon physics brings CDM and non-CDM predictions closer together. We have seen that baryons become relevant for scales $10^{8-15} M_\odot$, so they affect the halos in figure 10. Thus, although we cannot say that baryons explain all small-scale problems that arise from CDM, we can say that it aids in finding an allround theory.

References

[1] F. Zwicky. Die Rotverschiebung von extragalaktischen Nebeln. *Helv. Phys. Acta*, 6:110–127, 1933. [Gen. Rel. Grav.41,207(2009)].

[2] Vera C. Rubin and W. Kent Ford, Jr. Rotation of the Andromeda Nebula from a Spectroscopic Survey of Emission Regions. *Astrophys. J.*, 159:379–403, 1970.

[3] Jian Qi Shen. The dark-baryonic matter mass relation for observational... *Gen. Rel. Grav.*, 50(6):73, 2018.

[4] Mads T. Frandsen and Jonas Petersen. Investigating Dark Matter and MOND Models with Galactic Rotation Curve Data. 2018.

[5] KG Begeman, AH Broeils, and RH Sanders. Extended rotation curves of spiral galaxies: Dark haloes and modified dynamics. *Monthly Notices of the Royal Astronomical Society*, 249(3):523–537, 1991.

[6] J. Ehlers and P. Schneider. Gravitational lensing. In *Proceedings, 13th International Conference on General Relativity and Gravitation: Cordoba, Argentina, June 28-July 4, 1992*, pages 21–40, 1993.

[7] Douglas Clowe, Maruša Bradač, Anthony H Gonzalez, Maxim Markevitch, Scott W Randall, Christine Jones, and Dennis Zaritsky. A direct empirical proof of the existence of dark matter. *The Astrophysical Journal Letters*, 648(2):L109, 2006.

[8] Maxim Markevitch, AH Gonzalez, D Clowe, A Vikhlinin, W Forman, C Jones, S Murray, and W Tucker. Direct constraints on the dark matter self-interaction cross section from the merging galaxy cluster 1e 0657–56. *The Astrophysical Journal*, 606(2):819, 2004.

[9] Maxim Markevitch and Alexey Vikhlinin. Shocks and cold fronts in galaxy clusters. *Physics Reports*, 443(1):1–53, 2007.

[10] J. R. Brownstein and J. W. Moffat. The Bullet Cluster 1E0657-558 evidence shows Modified Gravity in the absence of Dark Matter. *Mon. Not. Roy. Astron. Soc.*, 382:29–47, 2007.

[11] Nathlia Cibirka et al. RELICS: Strong Lensing analysis of the galaxy clusters Abell S295, Abell 697, MACS J0025.4-1222, and MACS J0159.8-0849. 2018.

[12] Daniel J. Eisenstein et al. Detection of the Baryon Acoustic Peak in the Large-Scale Correlation Function of SDSS Luminous Red Galaxies. *Astrophys. J.*, 633:560–574, 2005.

[13] P. A. R. Ade et al. Planck 2015 results. XIII. Cosmological parameters. *Astron. Astrophys.*, 594:A13, 2016.

[14] M. Davis, G. Efstathiou, C. S. Frenk, and S. D. M. White. The evolution of large-scale structure in a universe dominated by cold dark matter. *apj*, 292:371–394, May 1985.

[15] Scott Dodelson and Lawrence M. Widrow. Sterile neutrinos as dark matter. *Phys. Rev. Lett.*, 72:17–20, Jan 1994.

[16] O. Lahav and A.R. Liddle. The Cosmological Parameters. 21, 2013.

[17] N. Fornengo. Dark matter overview. In *25th European Cosmic Ray Symposium (ECRS 2016) Turin, Italy, September 04-09, 2016*, 2016.

[18] R. D. Peccei and Helen R. Quinn. CP conservation in the presence of pseudoparticles. *Phys. Rev. Lett.*, 38:1440–1443, Jun 1977.

[19] John Preskill, Mark B. Wise, and Frank Wilczek. Cosmology of the invisible axion. *Physics Letters B*, 120(1):127 – 132, 1983.

[20] Michael Dine and Willy Fischler. The not-so-harmless axion. *Physics Letters B*, 120(1):137 – 141, 1983.

[21] A. Klypin, J. Holtzman, J. Primack, and E. Regos. Structure Formation with Cold plus Hot Dark Matter. *apj*, 416:1, October 1993.

[22] Joel R. Primack, Jon Holtzman, Anatoly Klypin, and David O. Caldwell. Cold + hot dark matter cosmology with $m(\nu_\mu) \approx m(\nu_\tau) \approx 2.4$ ev. *Phys. Rev. Lett.*, 74:2160–2163, Mar 1995.

[23] Benoit Famaey and Stacy McGaugh. Modified Newtonian Dynamics (MOND): Observational Phenomenology and Relativistic Extensions. *Living Rev. Rel.*, 15:10, 2012.

[24] Mordehai Milgrom. MOND-theoretical aspects. *New Astron. Rev.*, 46:741–753, 2002.

[25] Paul M. Chesler and Abraham Loeb. Constraining Relativistic Generalizations of Modified Newtonian Dynamics with Gravitational Waves. *Phys. Rev. Lett.*, 119(3):031102, 2017.

[26] B.P. Abbott et al. GW170817: Observation of Gravitational Waves from a Binary Neutron Star Inspiral. *Phys. Rev. Lett.*, 119(16):161101, 2017.

[27] S. Boran, S. Desai, E. O. Kahya, and R. P. Woodard. GW170817 Falsifies Dark Matter Emulators. *Phys. Rev.*, D97(4):041501, 2018.

[28] Irwin I. Shapiro. Fourth Test of General Relativity. *Phys. Rev. Lett.*, 13:789–791, 1964.

[29] Guy D. Moore and Ann E. Nelson. Lower bound on the propagation speed of gravity from gravitational Cherenkov radiation. *JHEP*, 09:023, 2001.

[30] Joshua W. Elliott, Guy D. Moore, and Horace Stoica. Constraining the new Aether: Gravitational Cerenkov radiation. *JHEP*, 08:066, 2005.

[31] B. P. Abbott et al. Observation of Gravitational Waves from a Binary Black Hole Merger. *Phys. Rev. Lett.*, 116(6):061102, 2016.

[32] Craig Lage and Glennys R Farrar. The bullet cluster is not a cosmological anomaly. *Journal of Cosmology and Astroparticle Physics*, 2015(02):038, 2015.

[33] Garry W Angus, Huan Yuan Shan, Hong Sheng Zhao, and Benoit Famaey. On the proof of dark matter, the law of gravity, and the mass of neutrinos. *The Astrophysical Journal Letters*, 654(1):L13, 2006.

[34] Zhe Chang, Ming-Hua Li, Xin Li, Hai-Nan Lin, and Sai Wang. Finslerian MOND versus the Strong Gravitational Lensing of the Early-type Galaxies. *Eur. Phys. J.*, C73:2550, 2013.

[35] Stacy S. McGaugh. A Novel Test of the Modified Newtonian Dynamics with Gas Rich Galaxies. *Phys. Rev. Lett.*, 106:121303, 2011. [Erratum: Phys. Rev. Lett.107,229901(2011)].

[36] Xin Li, Ming-Hua Li, Hai-Nan Lin, and Zhe Chang. Finslerian MOND vs. observations of Bullet Cluster 1E0657-558. *Mon. Not. Roy. Astron. Soc.*, 428(4):2939–2948, 2013.

[37] Zhe Chang, Ming-Hua Li, Xin Li, Hai-Nan Lin, and Sai Wang. Effects of spacetime anisotropy on the galaxy rotation curves. *Eur. Phys. J.*, C73:2447, 2013.

[38] Carlos S Frenk and Simon DM White. Dark matter and cosmic structure. *Annalen der Physik*, 524(9-10):507–534, 2012.

[39] Gianfranco Bertone and Dan Hooper. A history of dark matter. *arXiv preprint arXiv:1605.04909*, 2016.

[40] Erik Holmberg. On the clustering tendencies among the nebulae. ii. a study of encounters between laboratory models of stellar systems by a new integration procedure. *The Astrophysical Journal*, 94:385, 1941.

[41] Michael Kuhlen, Mark Vogelsberger, and Raul Angulo. Numerical Simulations of the Dark Universe: State of the Art and the Next Decade. *Phys. Dark Univ.*, 1:50–93, 2012.

[42] Carlos S. Frenk, Simon D. M. White, and Marc Davis. Nonlinear evolution of large-scale structure in the universe. *Astrophys. J.*, 271:417, 1983.

[43] Ya. B. Zeldovich, J. Einasto, and S. F. Shandarin. Giant Voids in the Universe. *Nature*, 300:407–413, 1982.

[44] A Dekel and SJ Aarseth. The spatial correlation function of galaxies confronted with theoretical scenarios. *The Astrophysical Journal*, 283:1–23, 1984.

[45] Simon DM White, CS Frenk, and Marc Davis. Clustering in a neutrino-dominated universe. *The Astrophysical Journal*, 274:L1–L5, 1983.

[46] John Huchra, Marc Davis, David Latham, and J Tonry. A survey of galaxy redshifts. iv-the data. *The Astrophysical Journal Supplement Series*, 52:89–119, 1983.

[47] PR Shapiro, C Struck-Marcell, and AL Melott. Pancakes and the formation of galaxies in a neutrino-dominated universe. *The Astrophysical Journal*, 275:413–429, 1983.

[48] YA B Zel'Dovich. Gravitational instability: An approximate theory for large density perturbations. *Astronomy and astrophysics*, 5:84–89, 1970.

[49] Matthew R. Buckley and Annika H. G. Peter. Gravitational probes of dark matter physics. 2017.